Research Square

Preprints are preliminary reports that have not undergone peer review.
They should not be considered conclusive, used to inform clinical practice,
or referenced by the media as validated information.

The Shigella flexneri virulence factor PhoN2 (apyrase) contributes to early autophagosome entrapment evasion

D. Scribano#

daniela.scribano@uniroma1.it

Sapienza University of Rome

C. Ambrosi#

San Raffaele University

F. Superti

Association for Research on Integrative Oncology Therapies, (ARTOI) Foundation

A. Tinari

Italian National Health Institute

L. Maurizi

Sapienza University of Rome

A. T. Palamara

Italian National Health Institute

L. Nencioni

Sapienza University of Rome

C. Longhi

Sapienza University of Rome

C. Zagaglia

European University of Rome

M. Nicoletti

Research Article

Keywords: Shigella flexneri, PhoN2, IcsA, IcsB, actin-based motility, LC3, autophagy, lysosome positioning

Posted Date: November 20th, 2026

DOI: https://doi.org/10.21203/rs.3.rs-11688862/v1

License: This work is licensed under a Creative Commons Attribution 4.0 International License.
Read Full License

Additional Declarations: No competing interests reported.

Abstract

Enterocytes represent the first line of defense against enteropathogens. Autophagy is a highly conserved cellular pathway mediating the degradation and recycling of damaged cellular components, including invasive pathogens, to maintain cell homeostasis and to restrict intracellular bacterial replication and spreading. However, *Shigella flexneri*, the etiological agent of bacillary dysentery, has evolved specific strategies to subvert and escape this innate immune response, primarily via its Type III Secretion System (T3SS) effectors, such as IcsB, which competitively binds IcsA (VirG), thereby preventing ATG5-mediated recognition. Herein, we report the contribution of the periplasmic virulence factor PhoN2 (a conserved ATP-diphosphohydrolase/apyrase encoded on the pINV plasmid) to the evasion from the autophagic pathway. We previously showed that PhoN2 is required for proper unipolar IcsA exposition and actin-based motility (ABM). In this study, using fluorescence microscopy, tandem mRFP-GFP/LC3 immunofluorescence reporter assays, and transmission electron microscopy (TEM), we demonstrate that, starting from the early stages of infection, a *phoN2* mutant is significantly decorated by LC3 at levels comparable to an *icsB* mutant, and it is entrapped within double-membrane autophagosomes and amphisomes. Furthermore, infection with the *phoN2* mutant induces intracellular lysosomal clustering in host cells, suggesting that the autophagic pathway proceeds to late stages. Altogether, these results demonstrate for the first time the involvement of PhoN2 in preventing early autophagic recognition and in modulating host lysosome positioning, likely through its crucial role in maintaining proper IcsA surface presentation and functional IcsA-IcsB interactions.

One-Sentence Summary

The *S. flexneri* periplasmic virulence factor PhoN2 is required for bacterial evasion from autophagy during the early stages of infection.

INTRODUCTION

Autophagy is an evolutionarily conserved catabolic pathway that allows eukaryotic cells to degrade and recycle old or damaged intracellular components by sequestering proteins and organelles into specialized double-membrane vesicles called autophagosomes, which subsequently fuse with lysosomes for degradation [1]. Recognized as an essential component of the host innate immune response, autophagy (specifically xenophagy) acts to restrict the replication and intracellular spreading of invasive bacterial pathogens [2]. While expressed at basal levels under nutrient-rich conditions to maintain cellular homeostasis (anabolic state), autophagy is rapidly upregulated in response to environmental stresses, nutrient scarcity (e.g., amino acid starvation), or microbial infections (catabolic state) [3]. Lysosomes, long viewed merely as terminal degradative organelles, are now recognized as dynamic signaling platforms central to multiple cellular functions, including pathogen killing, metabolic signaling, gene regulation, plasma membrane repair, and cell migration [4, 5]. Central to these functions is the master growth regulator mechanistic target of rapamycin complex 1 (mTORC1) [3, 4, 6]. Lysosome function strictly depends on their ability to move in a regulated "stop-and-go" manner and on their spatial

positioning within the host cytoplasm. Under nutrient-rich conditions, mTORC1 is active, and lysosomes are scattered throughout the cell periphery. Upon nutrient starvation or bacterial infection, mTORC1 is inactivated, shifting the cell to a catabolic state where lysosomes cluster in the perinuclear region thereby facilitating autophagosome-lysosome fusion [3, 4, 6].

To establish productive infections, facultative intracellular pathogens have evolved specific strategies to subvert or manipulate host autophagic surveillance [7]. *Shigella flexneri*, the causative agent of human bacillary dysentery, invades intestinal epithelial cells by bacterium-induced phagocytosis, rapidly lyses the primary phagocytic vacuole, and multiplies within the host cell cytoplasm [8]. *S. flexneri* intra- and intercellular spreading relies on the polarly exposed outer membrane autotransporter protein IcsA (VirG), which is necessary and sufficient for nucleating actin-based motility (ABM) by inducing unipolar actin polymerization [9–11]. Throughout the infection process, host cells trigger autophagic pathways via several mechanisms including, i) early recognition of ruptured vacuolar membrane fragments via galectins (e.g., Galectin-8) or glycans [12–14], ii) cytosolic detection by NOD-like receptors (NOD1/NOD2), which recruit ATG16L1 to bacterial entry sites [15]; iii) direct IcsA recognition by the autophagic protein ATG5, triggering LC3 recruitment and autophagosome formation around the bacterium [16]. Furthermore, IcsA-mediated actin polymerization recruits septin cage-like structures that entrap bacteria for ubiquitin- and LC3-dependent autophagy [17, 18]. Finally, recognition of secondary vacuoles leads to bacterial entrapment during cell-to-cell protrusion spreading [19]. To counteract this multi-tiered host defense, *S. flexneri* secretes specific effector proteins via its Type III Secretion System (T3SS) [20]. Prominent among these effectors is IcsB, which exhibits a triple mode of action. Early in infection, it inhibits LC3 recruitment to vacuolar membrane remnants by recruiting Toca-1 near intracellular bacteria, thereby preventing ubiquitination and autophagy adaptor engagement [14, 21]. Later, IcsB competitively binds IcsA, masking the ATG5-binding site on IcsA and preventing autophagosome formation [16]. During cell-to-cell spread, IcsB acts synergistically with VirA to inhibit LC3-mediated entrapment of secondary vacuoles [19].

S. flexneri encodes PhoN2 (apyrase) on the virulence plasmid (pINV), which is a highly conserved periplasmic ATP-diphosphohydrolase belonging to the family of non-specific bacterial acid phosphatases [22]. We previously demonstrated that PhoN2, independently of its catalytic activity, is required for the proper polar localization and exposition of IcsA at the old bacterial pole, which is critical for efficient ABM and plaque formation [23–26]. Indeed, *phoN2* mutants displayed an altered IcsA distribution, accompanied by aberrant actin clouds or short comet tails and severely impaired intercellular spread [24, 25]. Thus, the aim of this study was to evaluate whether PhoN2 could be involved in autophagy evasion in *S. flexneri*. Herein, we demonstrated that PhoN2 contributes to the ability of *S. flexneri* to escape autophagic recognition at early stages of infection. In particular, the *phoN2* mutant is more readily recognized by the autophagic machinery and becomes entrapped within autophagosomes. Furthermore, activation of autophagy in cells infected with the *phoN2* mutant is associated with marked lysosomal clustering, consistent with progression of the autophagic pathway towards the lysosomal compartment. However, this response does not significantly reduce intracellular

bacterial survival, suggesting that *S. flexneri* employs additional mechanisms to withstand lysosomal killing at later stages of infection.

MATERIALS AND METHODS

Bacterial strains and growth conditions

The bacterial strains used in this study are the *Shigella flexneri* WT strain M90T, the isogenic *phoN2* mutant strain HND115, the complemented strain HND115/pHND10 (carrying a functional *phoN2::HA* gene on plasmid pHND10) and the *icsB* mutant strain (used as a positive control for autophagic recognition and activation). Where indicated, strains were transformed with pGFP plasmid (a kind gift from G. Prosseda). *S. flexneri* colonies were routinely selected on Congo Red agar plates prior to growth in Luria-Bertani (LB) broth at 37°C with shaking. Bacteria were subcultured to log-phase (OD_{600} = 0.8) before infection experiments. When required, antibiotics were included at the following concentrations: ampicillin (Ap), 100 µg/mL; chloramphenicol (Cm), 30 µg/mL. L-arabinose was used at the final concentration of 0.016% to induce the expression of the fusion protein Apy-HA (Scribano et al., 2014).

Cell culture and infection assay

HeLa cells stably expressing the tandem fluorescent-tagged mRFP-GFP/LC3 reporter (a gift from M. Renna; [27, 28]), and Caco-2 intestinal epithelial cells were cultured in Dulbecco's modified Eagle's medium (DMEM) supplemented with 10% fetal bovine serum (FBS, Gibco, Thermo Scientific, Milan, Italy) and grown in the presence of 5% CO_2 at 37°C. mRFP-GFP/LC3 expressing HeLa cells were cultivated in the presence of 600 µg/mL of Geneticin (G418, Sigma). The tandem fluorescent mRFP-GFP/LC3 construct encodes a fusion protein consisting of monomeric Red Fluorescent Protein (mRFP) and Green Fluorescent Protein (GFP) linked to the N-terminus of human LC3 (microtubule-associated protein 1 light chain 3). This tandem reporter allows the monitoring of autophagic flux based on the differential pH sensitivity of GFP and mRFP; the GFP signal is quenched within the acidic environment of the autolysosome, whereas the mRFP signal remains stable [29]. Semi-confluent monolayers were infected using the gentamicin protection assay at a multiplicity of infection (MOI) of 100, as previously described [30]. After 45 min of incubation at 37°C to allow bacterial internalization, infected cells were extensively washed and incubated in fresh medium containing gentamicin 50 µg/mL for different time points (0.5, 1-, 2-, or 4-hours post-infection, HPI). To induce autophagy, cell monolayers were incubated in Hanks' Balanced Salt Solution (HBSS).

Fluorescence microscopy

For time-course LC3 decoration assay, mRFP-GFP/LC3-expressing HeLa cells were infected for 0.5, 1, and 2 HPI. At each time point, cells were washed, fixed with 4% (w/v) paraformaldehyde for 10 min, permeabilized with 0.2% Triton X-100 for 10 min, and blocked with 3% non-fat milk for 45 min. Cellular

nuclei and bacterial DNA were visualized by staining with 4',6-diamidino-2-phenylindole (DAPI; Molecular Probes). For lysosome positioning assay, HeLa cells were infected with pGFP-carrying *S. flexneri* strains for 2 and 4 HPI. Lysosomes were labeled by adding 0.1 µM LysoTracker Red DND-99 (Molecular Probes, Thermofisher, Italy) prior to analysis. Uninfected HeLa cells incubated in complete medium (CC) served as negative controls for autophagy, whereas uninfected cells incubated in HBSS served as positive controls for nutrient starvation-induced autophagy and lysosomal clustering.

Single and merged images were captured using a Leica DM5000B fluorescence microscope equipped with Digital FireWire Color (DFX350) and Black & White (DFX300) camera systems and processed using Leica Application Suite 2.7.0.R1 software, or analyzed via confocal microscopy. Signal overlaps around individual bacteria exhibiting LC3 recruitment were quantified from at least 300 cells per condition across three independent experiments.

Transmission Electron Microscopy (TEM)

Semi-confluent Caco-2 monolayers were infected for 4 HPI as described above. Monolayers were immediately fixed in 2.5% glutaraldehyde, 2% paraformaldehyde, and 2 mM $CaCl_2$ in 0.1 M sodium cacodylate buffer (pH 7.2). Fixed specimens were washed in cacodylate buffer, post-fixed with 1% osmium tetroxide in the same buffer for 1 h at room temperature, washed, dehydrated through a graded ethanol series (30% to 100%), and embedded in Agar 100 (Agar Scientific Ltd., UK). Ultrathin sections obtained with an MT-2B Ultramicrotome (LKB-Pharmacia) were stained with uranyl acetate and lead citrate and examined using a Philips 208S transmission electron microscope. Approximately 200 independent fields were analyzed per sample.

Statistical analysis

Normal distribution was determined by the Shapiro–Wilk test. The statistical differences of normally distributed data were analyzed by two-way ANOVA by using GraphPad Prism 10.00 software (San Diego, USA). Values of $P < 0.05$ were taken as being statistically significant. Data are expressed as the mean ± standard deviation (SD) of at least three independent experiments.

RESULTS

PhoN2 participates to S. flexneri evasion from the autophagic pathway

To evaluate whether PhoN2 contributes to the evasion of *S. flexneri* from autophagic recognition, we performed time-course infection experiments using HeLa cells stably expressing the tandem mRFP-GFP/LC3 reporter [27, 28]. Cells were infected with strains M90T, HND115, HND115/pHND10, and the *icsB* mutant, used as positive control for autophagy activation. The percentage of LC3-decorated intracellular bacteria was quantified at 0.5, 1, and 2 HPI (Fig. 1). Results demonstrated that HND115 was significantly more associated with mRFP-GFP/LC3 signal than M90T and the complemented

HND115/pHND10 strains at all time points tested ($p < 0.05$; Fig. 1). At 1 and 2 HPI, the percentage of LC3-decorated M90T remained low (15.8% and 16.7%, respectively), whereas HND115 displayed a significantly higher percentage of LC3 decoration (28.7% and 28.5%, respectively). Complementation with pHND10 rescued the mutant phenotype, restoring LC3 decoration levels to those of the WT strain (18.7% at 2 HPI). As expected, the *icsB* mutant exhibited significant high levels of LC3 decoration throughout the time course (32.5% at 2 HPI). Interestingly, no statistically significant differences in LC3-decorated bacteria were observed between HND115 and the *icsB* mutant at 1 and 2 HPI (Fig. 1). Even as early as 0.5 HPI, LC3 decoration of HND115 was significantly higher than that of both WT and the complemented strains. Microscopic observation revealed that LC3 appeared as a continuous signal completely surrounding the *phoN2* defective bacteria, rather than punctate foci, suggesting direct targeting of cytosolic bacteria rather than isolated vacuolar remnants. These data demonstrated that PhoN2 is required for *S. flexneri* evasion from autophagic recognition from the very early stages of infection (0.5 HPI). Interestingly, the mRFP-GFP/LC3 reporter indicated no GFP quenching at 2 HPI, suggesting that lysosomal fusion had not yet occurred at this time point.

S. flexneri phoN2 mutant is actively entrapped into autophagosomes in Caco-2 cells

To confirm autophagic entrapment at the ultrastructural level, Caco-2 intestinal epithelial cells were infected with strains M90T, HND115 and HND115/pHND10 for 4 h and autophagosome-entrapped bacteria were visualized and quantified by transmission electron microscopy (Fig. 2). At 4 HPI, M90T was detected freely in the cell cytoplasm and only rarely within single-membrane compartments. Moreover, some bacteria were associated with actin tails, indicating active ABM (Fig. 2). As expected, the complemented strain was found to be both free in cell cytoplasm and sometimes associated with actin tails (Fig. 2). Vice versa, HND115 was frequently enclosed within double membrane vesicles characteristic of autophagosomes. Furthermore, cells infected with HND115 showed amphisomes containing several bacterial cells (Fig. 2). As expected, this mutant completely lacked well-defined polar actin comet tails. These results demonstrate that Caco-2 cells activate an enhanced autophagic response against the *phoN2* mutant in comparison with those infected with the WT and complemented strains (Fig. 2). Moreover, the visualization of amphisome-containing bacteria further suggests that the autophagic pathway had proceeded to autophagosome-late endosome fusion.

Activation of autophagy against the phoN2 mutant induces intracellular lysosome clustering

To evaluate if autophagic entrapment of the *phoN2* mutant leads to lysosomal-mediated bacterial degradation, we analyzed both lysosomal distribution and intracellular bacterial survival in infected epithelial cells. Indeed, lysosomal positioning and clustering influences autophagosome formation and autophagosome-lysosome fusion rates [4]. HeLa cells were infected with strains M90T, HND115 and HND115/pHND10 for 2 and 4 h. Uninfected cells grown in complete medium (CC) were used as a negative control, while uninfected cells maintained in HBSS served as a positive control for starvation-induced autophagy (Fig. 3A). At each time point, cells were washed, and stained with LysoTracker DND-99 dye, to visualize lysosomes in red, while bacteria, carrying the pGFP plasmid were marked in green.

Parallel infected cultures were used for intracellular bacteria counts in order to evaluate if activation of the degradation pathway could result in intracellular bacterial clearance. As expected, uninfected HeLa cells cultured in complete medium exhibited lysosomes scattered throughout the cytoplasm (Fig. 3A, CC). Conversely, uninfected cells subjected to HBSS starvation displayed pronounced lysosomal clustering (Fig. 3A, HBSS). Cells infected with M90T or HND115/pHND10 maintained a scattered lysosomal pattern comparable to nutrient-rich control cells (Fig. 3B). Vice versa, cells infected with HND115 displayed marked lysosomal clustering (Fig. 3B), closely resembling the pattern of starved uninfected cells (Fig. 3A, HBSS).

Despite this lysosomal clustering, a direct co-localization between HND115 and LysoTracker-stained acidic compartments was not observed at either time point. Furthermore, intracellular bacterial counts demonstrated no significant reduction in HND115 survived cells compared with WT at both time points (data not shown). These results indicate that, although loss of PhoN2 triggers host lysosomal repositioning and early autophagosomal entrapment, it does not lead to an intracellular bacterial clearance at these time points.

DISCUSSION

Enterocytes represent the primary physical and immunological barrier against enteropathogens. Host cells utilize autophagy as an ancient, highly conserved innate defense mechanism to restrict intracellular microbial proliferation [31]. *S. flexneri* has evolved sophisticated countermeasures to manipulate this machinery. In this study, we identify the periplasmic ATP-diphosphohydrolase PhoN2 as a novel contributor to *S. flexneri* autophagic evasion. To escape autophagy, *S. flexneri* relies on the T3SS effector IcsB, which acts at multiple stages: masking IcsA from ATG5 recognition, preventing LC3 recruitment to vacuolar membrane remnants via Toca-1 interaction, and inhibiting secondary vacuole entrapment [14, 16, 19]. We previously established that PhoN2 is necessary for the proper polar localization and exposition of IcsA on the outer membrane, as its absence severely altered IcsA exposition, impaired actin tail assembly and intracellular spread [23–25]. Our current findings show that a *phoN2* mutant is efficiently recognized by the autophagic machinery at levels comparable to *icsB* mutant. TEM analysis corroborated these findings, revealing double-membrane autophagosome entrapment and amphisome formation surrounding *phoN2* mutant in Caco-2 cells. The autophagic pathway activation against the *phoN2* mutant is linked with PhoN2 established role in IcsA proper exposition, which is required for ABM [24, 25]. Indeed, ABM itself serves as an autophagy evasion strategy, as demonstrated in *Listeria monocytogenes, Rickettsia parkeri* and *Burkholderia thailandensis*, and *Mycobacterium marinum* [32]. In particular, despite both IcsA of *S. flexneri* and ActA of *L. monocytogenes* are directly recognized by the autophagic machinery, these pathogens adopted different molecular mechanism to overcome autophagic entrapment. ActA, by interacting with Ena/VASP complex and activating actin polymerization masks itself from the autophagic adaptors p62/NDP52 [33]. Viceversa, the ATG5-binding residues of IcsA are masked by IcsB binding [16]. Differently, in *R. parkeri* and *B. pseudomallei* the ABM-driving proteins RickA and BimA, respectively, are not directly targeted by autophagy and ABM represents a further way to avoid the assembly of ubiquitin ligases on conserved bacterial surface structures, such as

OmpA, the T3SS and O antigen [34]. Hence, in *S. flexneri* the combined roles of PhoN2 and IcsB in controlling IcsA surface exposition ensure efficient ABM and autophagic evasion.

An intriguing finding of this study is that infection with the *phoN2* mutant induces striking intracellular lysosomal clustering, a physiological state characteristic of amino acid starvation and mTORC1 inactivation [3, 4]. Invasive pathogens induce host metabolic stress, and intracellular *Shigella* infection triggers an amino acid starvation response that activates autophagosome formation and lysosomal repositioning [3]. Beyond starvation, lysosome acidification can be promoted through the endolysosomal ATP-sensitive Na+ channel (lysoNaATP), an ATP sensor localized on the lysosomal membrane. Indeed, during cell starvation, the drop of ATP levels causes mTOR dissociation from the lysosomal membrane, and the opening of the lysoNaATP, thereby allowing Na^+ and other ions to exit the lysosome and accelerating lysosome-dependent clearance. Hence, the lysoNaATP channel links lysosomal control of nutrient recycling to the mTOR signaling network that monitors nutrients availability and responds to nutrient depletion [35, 36]. We previously demonstrated that *S. flexneri* is capable to maintain a physiological intracellular ATP pool trough cytoplasmic release of PhoN2 in infected cells, which might contribute to inhibit lysosomal activation. Vice versa, the lack of PhoN2 causes an increase of intracellular ATP levels, resulting in the NLRP3 inflammasome activation and cell death [26]. Active inflammasomes are targeted to lysosomal degradation as a negative feedback mechanism that limits exaggerated inflammatory response [37]. It can be speculated that cells infected with the *phoN2* mutant integrate two main signals leading to lysosomal repositioning, the autophagic bacterial entrapment and the inflammasome activation.

Interestingly, despite increased autophagosomal entrapment and lysosomal clustering, the *phoN2* mutant did not exhibit reduced intracellular bacterial counts up to 4 HPI. This is consistent with observations by Baxt and Goldberg [14], who described that early LC3 recruitment around *S. flexneri* does not immediately target bacteria to degradative destruction or affect short-term survival. At later stages of infection, other mechanisms may occur to support bacterial intracellular survival. In this context, it was demonstrated that *S. flexneri* is capable to overall subvert vesicles intracellular trafficking through the T3SS effectors IpaJ and VirA, thereby allowing a more efficient intracellular replication [38]. In addition, IpaH4.5 disrupts the mannose-6-phosphate receptor-dependent lysosomal trafficking and function, thereby counteracting lysosomal degradation [39].

In conclusion, this work demonstrates that the periplasmic protein PhoN2, beyond its known role in IcsA surface exposition and ABM, indirectly enables *S. flexneri* to evade early autophagic entrapment. This result further underlines the huge complexity of *S. flexneri* manipulation of host innate defenses. Future studies will evaluate the molecular interactions among PhoN2, IcsA, and IcsB at the bacterial outer membrane and will clarify the mechanism by which *S. flexneri* modulates lysosomal trafficking within intestinal epithelial cells.

Declarations

ACKNOWLEDGEMENTS

We dedicate this work to the memory of our co-author, mentor, colleague and friend Mauro Nicoletti, who passed away before this publication. Professor Mauro Nicoletti was the driving force behind this project; his vision, intellectual depth, and dedication were fundamental to the conception and realization of this study. His absence is deeply felt by us all, and this work stands as a testament to this scientific legacy.

We thank Professor Abdelmounaaim Allaoui for providing the *icsB* mutant strain, Dr. M. Renna for providing the mRFP-GFP/LC3 stably expressing HeLa cells, Prof. Gianni Prosseda for providing the pGFP plasmid, and Dr. Giovanniluigi Buglia for technical support with confocal microscopy.

Author contribution

Author contributions: Conceptualization: MN; Methodology: MN, DS, CA, FS, AT, CZ; Validation: DS, CA, FS, AT, CZ; Investigation: DS, CA, FS, AT; Formal analysis: DS, CA, FS, AT; Resources: MN, DS, FS, CZ, CL, LN, ATP; Visualization: DS, CA, FS, AT; Writing original draft: MN, DS, CA, FS; Writing—review editing: MN, DS, CA, FS, AT, LM, ATP, CZ, CL, LN Supervision: MN, CA, FS. All authors have read and agreed to publish this version of the manuscript.

FUNDING

This work was partially supported by Sapienza Ateneo fundings (Progetto dipartimentale RD12318AAC3B4A3E) to DS.

CONFLICT OF INTEREST

The authors declare that they have no conflicts of interest.

References

1. Mao K, Klionsky DJ (2016) Xenophagy: A special form of autophagy for microbe clearance. Rev Physiol Biochem Pharmacol 172:1–25. https://doi.org/10.1007/112_2015_27
2. Günther J, Seyfert HM (2018) The first line of defence: insights into the innate immune response of mammary epithelial cells to pathogens. Dev Comp Immunol 84:150–165. https://doi.org/10.1016/j.dci.2018.02.016
3. Tattoli I, Sorbara MT, Vuckovic D, Ling A, Soares F, Carneiro LAM, Yang C, Girardin SE (2012) Amino acid starvation induced by invasive bacterial pathogens triggers an innate host defense program. Cell Host Microbe 11:563–575. https://doi.org/10.1016/j.chom.2012.04.012
4. Korolchuk VI, Saiki S, Lichtenberg M, Siddiqi FH, Roberts EA, Imarisio S, Jahrling JR, Sarkar S, Futter CE, Menzies FM, O'Kane CJ, Deretic V, Rubinsztein DC (2011) Lysosomal positioning coordinates cellular nutrient responses. Nat Cell Biol 13:453–460. https://doi.org/10.1038/ncb2241

5. Ballabio A, Bonifacino JS (2020) Lysosomes as dynamic regulators of cell and organismal homeostasis. Nat Rev Mol Cell Biol 21:101–118. https://doi.org/10.1038/s41580-019-0185-4
6. Chowdhury I, Siregar TAP, Haque MF, Ponpuak M (2026) The final gate: bacterial subversion of autophagosome-lysosome fusion as a conserved immune evasion strategy. Crit Rev Microbiol 52:377–393. https://doi.org/10.1080/1040841X.2025.2562930
7. Krokowski S, Mostowy S (2016) Bacterial autophagy in host defense and intracellular pathogenesis. J Mol Biol 428:2175–2185. https://doi.org/10.1016/j.jmb.2016.03.024
8. Schnupf P, Sansonetti PJ (2019) Shigella pathogenesis: new insights through advanced methodologies. Microbiol Spectr 7. https://doi.org/10.1128/microbiolspec.BAI-0023-2019. :BAI-0023-2019
9. Goldberg MB, Theriot JA (1995) Shigella flexneri surface protein IcsA is sufficient to direct actin-based motility. Proc Natl Acad Sci USA 92:6572–6576. https://doi.org/10.1073/pnas.92.14.6572
10. Steinhauer J, Agha R, Pham T, Varga AW, Goldberg MB (1999) The unipolar Shigella surface protein IcsA is targeted directly to the bacterial old pole: IcsP cleavage of IcsA occurs over the entire bacterial surface. Mol Microbiol 32:367–377. https://doi.org/10.1046/j.1365-2958.1999.01361.x
11. Lamason RL, Welch MD (2017) Actin-based motility and cell-to-cell spread of bacterial pathogens. Curr Opin Microbiol 35:48–57. https://doi.org/10.1016/j.mib.2016.11.007
12. Dupont N, Lacas-Gervais S, Bertout J, Paz I, Freche B, Van Nhieu GT, van der Goot FG, Sansonetti PJ, Lafont F (2009) Shigella phagocytic vacuolar membrane remnants participate in the cellular response to pathogen invasion and are regulated by autophagy. Cell Host Microbe 6:137–149. https://doi.org/10.1016/j.chom.2009.07.005
13. Thurston TLM, Wandel MP, von Muhlinen N, Foeglein A, Randow F (2012) Galectin 8 targets damaged vesicles for autophagy to defend cells against bacterial invasion. Nature 482:414–418. https://doi.org/10.1038/nature10744
14. Baxt WG, Goldberg MB (2014) Host Toca-1 mediates Shigella avoidance of autophagy. Cell Host Microbe 15:466–477. https://doi.org/10.1016/j.chom.2014.03.008
15. Travassos LH, Carneiro LAM, Ramjeet M, Hussey S, Kim YG, Magalhaes JG, Yuan L, Soares F, Cheoa E, Le Bourhis L, Boneca IG, Allaoui A, Jones NL, Nuñez G, Philpott DJ, Girardin SE (2010) Nod1 and Nod2 direct autophagy by recruiting ATG16L1 to the plasma membrane at the site of bacterial entry. Nat Immunol 11:55–62. https://doi.org/10.1038/ni.1823
16. Ogawa M, Yoshimori T, Suzuki T, Sagara H, Mizushima N, Sasakawa C (2005) Escape of intracellular Shigella from autophagy by IcsB. Science 307:727–731. https://doi.org/10.1126/science.1106036
17. Mostowy S, Bonazzi M, Hamon MA, Tham TN, Mallet A, Lecomte P, Gounero L, Bichat F, Gouin E, Cossart P (2010) Entrapment of intracytoplasmic Shigella by septin cages in airway epithelial cells. Cell Host Microbe 8:433–444. https://doi.org/10.1016/j.chom.2010.10.009
18. Mostowy S, Sancho-Shimizu V, Hamon MA, Simeone R, Brosch R, Johansen T, Cossart P (2011) p62 and NDP52 cooperate to target intracytoplasmic Shigella and Listeria to autophagy. J Biol Chem 286:26987–26995. https://doi.org/10.1074/jbc.M111.230979

19. Campbell-Valois FX, Sachse M, Sansonetti PJ, Parsot C (2015) Escape of Shigella flexneri from vacuolar remnants requires VirA and IcsB. Nat Commun 6:7391. https://doi.org/10.1038/ncomms8391
20. Bajunaid W, Haidar-Ahmad N, Kottarampatel AH, Ourida Manigat F, Silué N, Tchagang CF, Tomaro K, Campbell-Valois FX (2020) The T3SS of Shigella: expression, structure, function, and role in vacuole escape. Microorganisms 8:1933. https://doi.org/10.3390/microorganisms8121933
21. Leung Y, Ally S, Goldberg MB (2008) Bacterial actin assembly requires Toca-1 to relieve N-WASP autoinhibition. Cell Host Microbe 3:39–47. https://doi.org/10.1016/j.chom.2007.11.004
22. Berlutti F, Casalino M, Zagaglia C, Fradiani PA, Visca P, Nicoletti M (1998) Expression of the virulence plasmid-carried apyrase gene (apy) of enteroinvasive Escherichia coli and Shigella flexneri is under the control of H-NS and the VirF and VirB regulatory cascade. Infect Immun 66:4957–4964. https://doi.org/10.1128/IAI.66.10.4957-4964.1998
23. Santapaola D, Casalino M, Petrucca A, Presutti C, Zagaglia C, Colonna B, Nicoletti M (2002) Enteroinvasive Escherichia coli virulence plasmid-carried apyrase (apy) and ospB genes are organized as a bicistronic operon and are subjected to differential expression. Microbiology 148:2519–2529. https://doi.org/10.1099/00221287-148-8-2519
24. Santapaola D, Del Chierico F, Petrucca A, Uzzau S, Casalino M, Colonna B, Sessa R, Nicoletti M (2006) Apyrase, the product of the virulence plasmid-encoded phoN2 (apy) gene of Shigella flexneri, is necessary for proper unipolar IcsA localization and for efficient intercellular spread. J Bacteriol 188:1620–1627. https://doi.org/10.1128/JB.188.5.1620-1627.2006
25. Scribano D, Petrucca A, Pompili M, Ambrosi C, Bruni E, Superti F, Nicoletti M (2014) Polar localization of PhoN2, a periplasmic Apyrase involved in Shigella flexneri virulence. PLoS ONE 9:e86394. https://doi.org/10.1371/journal.pone.0086394
26. Perruzza L, Zagaglia C, Vitiello L, Sarshar M, Strati F, Pasqua M, Grassi F, Nicoletti M, Palamara AT, Ambrosi C, Scribano D (2023) The Shigella flexneri virulence factor apyrase is released inside eukaryotic cells to hijack host cell fate. Microbiol Spectr 11:e0077523. https://doi.org/10.1128/spectrum.00775-23
27. Renna M, Schaffner C, Brown K, Shang S, Tamimi O, Rubinsztein DC (2010) Azithromycin blocks autophagy and may impair lysosomal clearance in mucosal epithelial cells. J Antimicrob Chemother 65:1485–1487. https://doi.org/10.1093/jac/dkq123
28. Zhou C, Zhong W, Zhou J, Sheng F, Fang Z, Wei Y, Wang Y (2012) Monitoring autophagic flux with mRFP-GFP-LC3 reporter in HeLa cells. Autophagy 8:1215–1223. https://doi.org/10.4161/auto.20702
29. Lopez A, Fleming A, Rubinsztein DC (2018) Seeing is believing: methods to monitor vertebrate autophagy in vivo. Open Biol 8:180106. https://doi.org/10.1098/rsob.180106
30. Ambrosi C, Pompili M, Scribano D, Limongi D, Petrucca A, Cannavacciuolo S, Schippa S, Zagaglia C, Grossi M, Nicoletti M (2015) The Shigella flexneri OspB effector: an early immunomodulator. Int J Med Microbiol 305:75–84. https://doi.org/10.1016/j.ijmm.2014.11.004

31. Sharma V, Verma S, Seranova E, Sarkar S, Kumar D (2018) Selective autophagy and xenophagy in infection and disease. Front Cell Dev Biol 6:147. https://doi.org/10.3389/fcell.2018.00147
32. Choe JE, Welch MD (2016) Actin-based motility of bacterial pathogens: mechanistic diversity and its impact on virulence. Pathog Dis 74:ftw099. https://doi.org/10.1093/femspd/ftw099
33. Yoshikawa Y, Ogawa M, Hain T, Yoshida M, Fukumatsu M, Kim M, Mimuro H, Nakagawa I, Yanagawa T, Ishii T, Kakizuka A, Sztul E, Chakraborty T, Sasakawa C (2009) Listeria monocytogenes ActA-mediated escape from autophagic recognition. Nat Cell Biol 11:1233–1240. https://doi.org/10.1038/ncb1967
34. Cheng MI, Chen C, Engström P, Portnoy DA, Mitchell G (2018) Actin-based motility allows Listeria monocytogenes to avoid autophagy in the macrophage cytosol. Cell Microbiol 20:e12854. https://doi.org/10.1111/cmi.12854
35. Laplante M, Sabatini DM (2012) mTOR signaling in growth control and disease. Cell 149:274–293. https://doi.org/10.1016/j.cell.2012.03.017
36. Cang C, Zhou Y, Navarro B, Seo YJ, Aranda K, Shi L, Battaglia-Hsu S, Nissim I, Clapham DE, Ren D (2013) mTOR regulates lysosomal ATP-sensitive two-pore Na(+) channels to adapt to metabolic state. Cell 152:778–790. https://doi.org/10.1016/j.cell.2013.01.023
37. Que X, Zheng S, Song Q, Pei H, Zhang P (2023) Fantastic voyage: the journey of NLRP3 inflammasome activation. Genes Dis 11:819–829. https://doi.org/10.1016/j.gendis.2023.01.009
38. Ferrari ML, Malardé V, Grassart A, Salavessa L, Nigro G, Descorps-Declere S, Rohde JR, Schnupf P, Masson V, Arras G, Loew D, Sansonetti PJ, Sauvonnet N (2019) Shigella promotes major alteration of gut epithelial physiology and tissue invasion by shutting off host intracellular transport. Proc Natl Acad Sci USA 116:13582–13591. https://doi.org/10.1073/pnas.1902922116
39. Sun J, Wang X, Lin H, Wan L, Chen J, Yang X, Li D, Zhang Y, He X, Wang B, Dong M, Zhong H, Wei C (2021) Shigella escapes lysosomal degradation through inactivation of Rab31 by IpaH4.5. J Med Microbiol 70:001382. https://doi.org/10.1099/jmm.0.001382

Figures

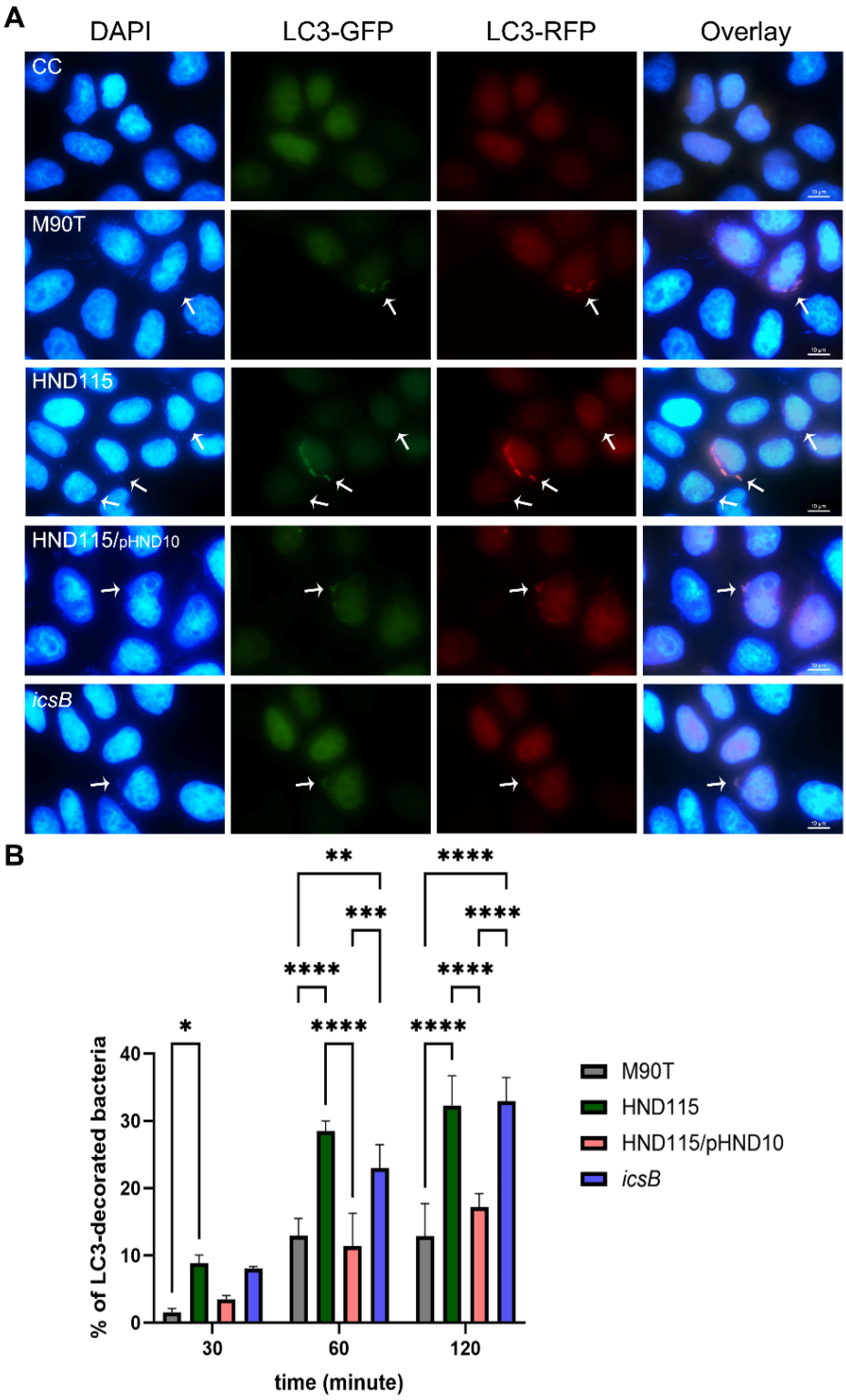

Figure 1

The *phoN2* mutant is decorated by LC3 at the early stages of infection. HeLa cells stably expressing the tandem mRFP-GFP/LC3 reporter were infected with M90T, HND115, HND115/pHND10 and the *icsB* mutant strains at an MOI of 100 for 0.5, 1, and 2 HPI. A) Representative fluorescence images of LC3-decorated bacteria visualized in green and red channels, as well as merged overlays. Arrows indicate LC3-decorated bacteria. Cellular and bacterial DNA were stained with DAPI (blue). B) Quantification of

LC3-decorated bacteria Data represent the mean ± SD of three independent experiments (at least 300 cells per strain per experiment were counted) Scale bar: 10 μm. Statistical significance was assessed using two-way ANOVA; *p < 0.05, **p < 0.01, ***p < 0.001, ****p < 0.0001.

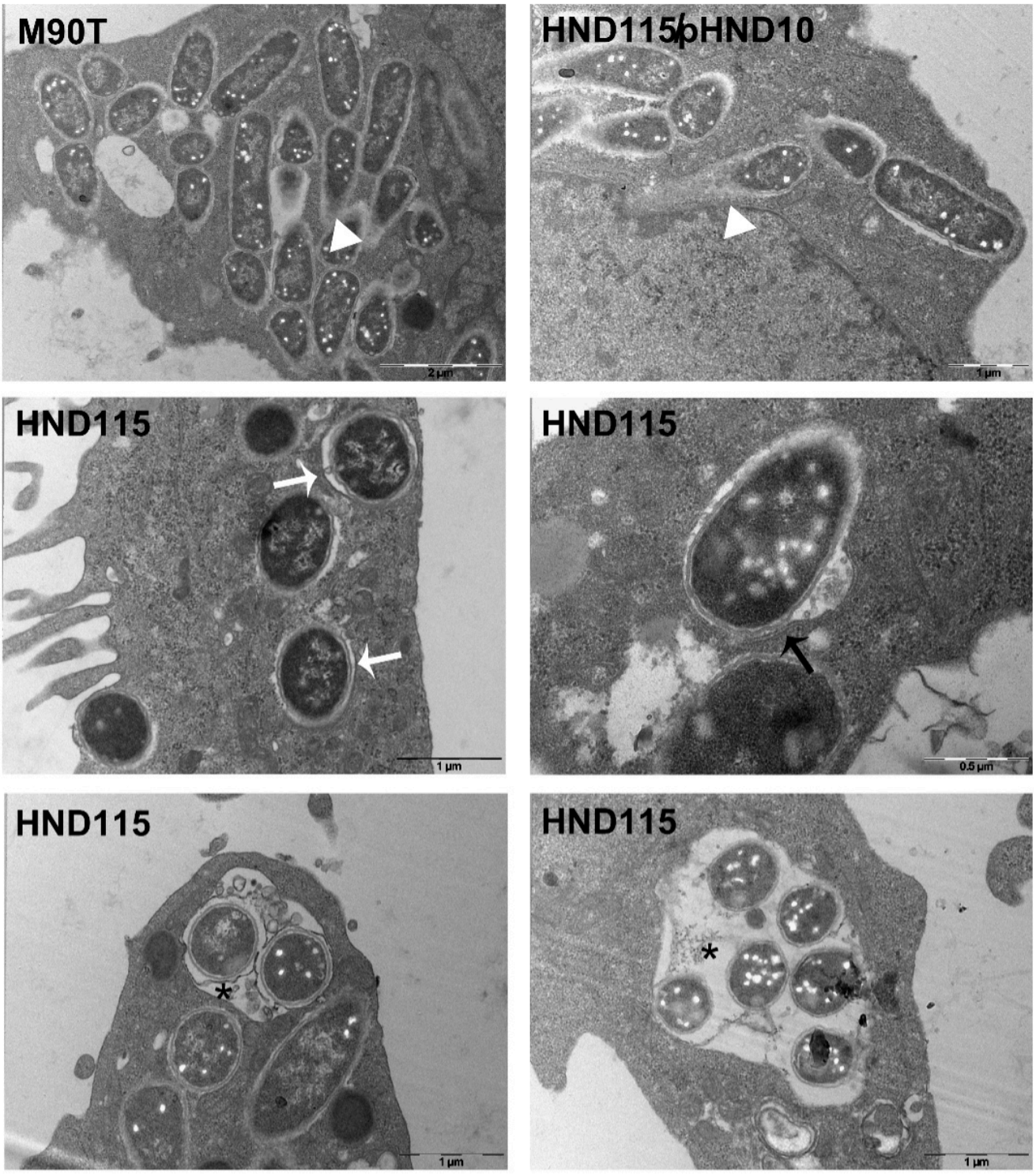

Figure 2

The *phoN2* mutant is entrapped within autophagosomes. Caco-2 intestinal epithelial cells were infected with M90T, HND115 and HND115/pHND10 strains for 4 h, fixed, and processed for TEM. Arrowheads indicate bacteria associated with polar actin comet tails. White arrows point to bacteria enclosed in single-membrane primary vacuoles. Black arrows indicate bacteria enclosed within double-membrane autophagosomes with characteristic lamellar structures. Black asterisks indicate bacteria enclosed in amphisomes containing late endosomal vesicles. Scale bars: 2 μm, 1 μm, and 0.5 μm.

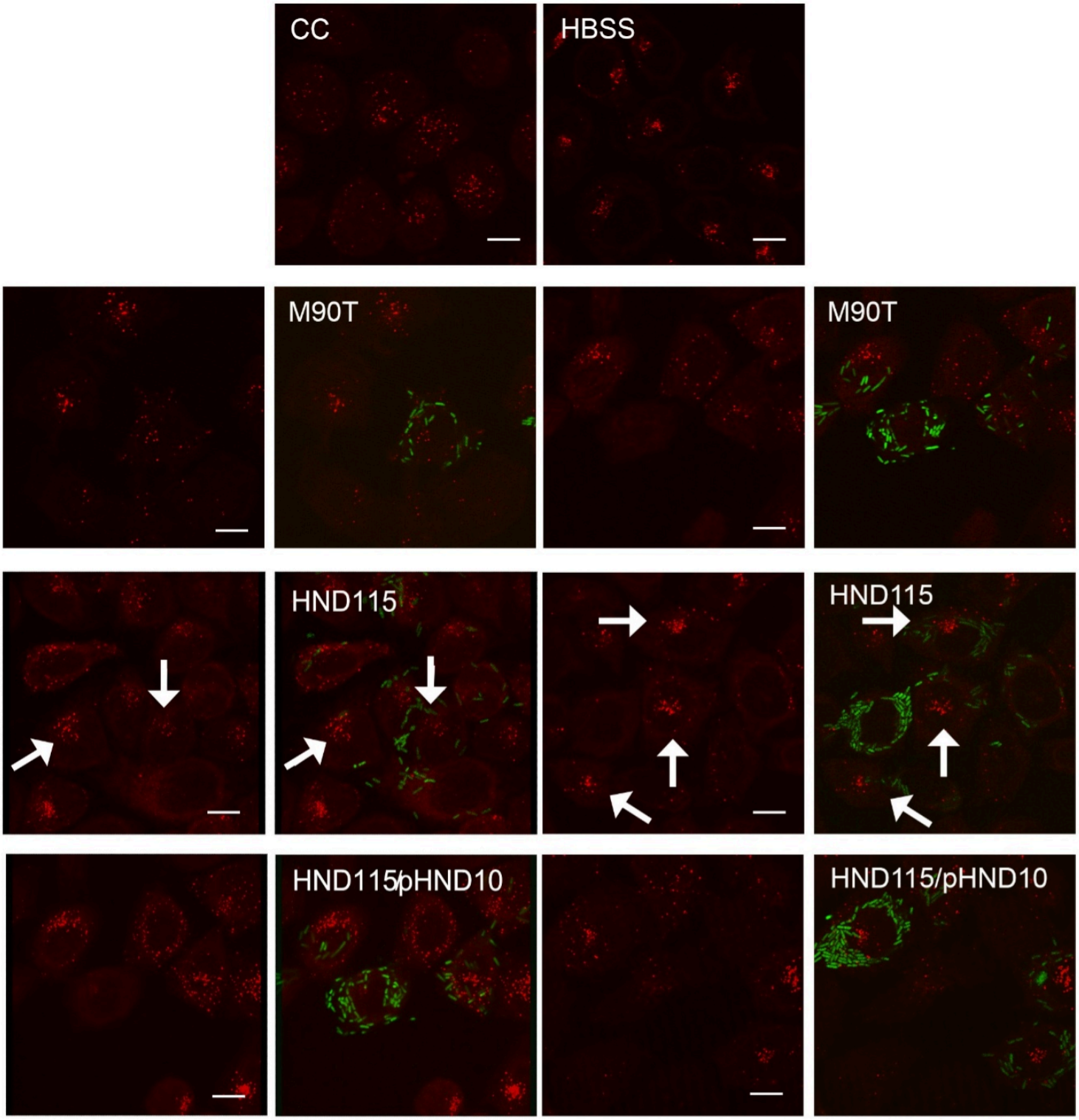

Figure 3

The *phoN2* mutant induces intracellular lysosome clustering. HeLa cells were infected with the GFP-expressing-M90T, HND115, and HND115/pHND10 strains at an MOI of 100 and analyzed at 2 and 4 HPI. Lysosomes were stained with LysoTracker Red DND-99 (red) and bacteria are visualized in green. A) Representative fluorescence images of control cells (CC) and starved cells (HBSS). B) Representative fluorescence images of infected cells at 2 and 4 HPI. Arrows point clustered lysosomes. Scale bar: 10 μm